Computational Limit Analysis for anchors and retaining walls

Jose J Muñoz[1], Andrei V Lyamin[2], Antonio Huerta[1]

[1]Departament MA3 e-mail: j.munoz@upc.edu, antonio.huerta@upc.edu
[2]Centre for Geotechnical and Materials Modelling

Keywords: Limit analysis, stability, retaining walls, bounds

Abstract: *The computation of the bearing capacity of engineering structures commonly relays on results obtained for simple academic examples. Recent developments in computational limit analysis have allowed engineers to compute bounds of the bearing capacity of arbitrary geometries. We here extend these formulations to problems with practical interest such as retaining walls, anchors, or excavations with particular interface conditions. These situations require the special treatment of the contact conditions between different materials, or the modelling of joints and anchors. We demonstrate the potential of the resulting tool with some practical examples.*

1. INTRODUCTION

According to the lower bound theorem of limit analysis, the bearing capacity of a structure is equal to the maximum load factor λ^* under equilibrium conditions and with admissible stresses σ. Formally, it can be computed as the optimal solution of the following maximisation problem [1]:

$$\lambda^* = \max \lambda$$
$$s.t. \begin{cases} a(\boldsymbol{v},\boldsymbol{\sigma}) + b(\boldsymbol{v},\boldsymbol{\sigma}) = \ell(\boldsymbol{v}), & \forall \boldsymbol{v} \\ \boldsymbol{\sigma} \in \mathcal{B} \end{cases} \tag{1}$$

The linear form *l(v),* and the bilinear forms $b(\boldsymbol{v},\boldsymbol{\sigma})$ and $a(\boldsymbol{v},\boldsymbol{\sigma})$ represent respectively the dissipation energy at the region where the velocity *v* is discontinuous (denoted Γ) and where it is continuos (denoted by Ω\Γ). These forms are explicitly given by,

$$a(\boldsymbol{v},\boldsymbol{\sigma}) := \int_{\Omega\backslash\Gamma} \boldsymbol{\varepsilon}(\boldsymbol{v}) : \boldsymbol{\sigma} \mathrm{d}\Omega$$
$$b(\boldsymbol{v},\boldsymbol{\sigma}) := \int_{\Gamma} [\![\boldsymbol{v}]\!] \cdot \boldsymbol{\sigma}\boldsymbol{n} \mathrm{d}\Gamma = \int_{\Gamma} [\![\boldsymbol{v}]\!] \bar{\otimes} \boldsymbol{n} : \boldsymbol{\sigma} \mathrm{d}\Gamma$$
$$\ell(\boldsymbol{v}) := \int_{\Omega} \boldsymbol{v} \cdot \boldsymbol{f} \mathrm{d}\Omega + \int_{\partial\Omega} \boldsymbol{v} \cdot \boldsymbol{g} \mathrm{d}\Gamma,$$

with $\boldsymbol{\varepsilon}(\boldsymbol{v})$ the strain rate tensor. The vectors $\boldsymbol{f}$ and $\boldsymbol{g}$ represent the body and boundary loads on the domain Ω. The symbol [[**v**]] denotes the jump of the velocity vector **v**. The optimisation problem in (1) has associated a dual optimisation problem, which is given by,

$$\lambda^* = \min_{\boldsymbol{v}} D(v)$$
$$s.t. \begin{cases} \ell(v) = 1 \\ -\varepsilon(\boldsymbol{v}) \in \mathcal{B}^* \\ -[\![v]\!]\bar{\otimes}\boldsymbol{n} \in \mathcal{B}^* \end{cases} \quad (2)$$

where B^* is the dual set to B which is defined by $B^*=\{\boldsymbol{s} \mid \boldsymbol{s}: \boldsymbol{\sigma}, \forall\, \boldsymbol{\sigma} \in B\}$.

2. LOWER AND UPPER BOUND FORMULATIONS

The particular saddle point structure of limit analysis allows us to use specific interpolation spaces ($\boldsymbol{\sigma}^{UB}$,$\boldsymbol{v}^{UB}$) and ($\boldsymbol{\sigma}^{LB}$,$\boldsymbol{v}^{LB}$) of the stresses and the velocities that yied upper and lower bounds of the optimal factor λ^*, denoted respectively by λ^{UB} and λ^{LB} . The details of the choices for the lower and upper bound problem may be found in [2]. We just mention that in the lower bound problem, the stresses $\boldsymbol{\sigma}^{LB}$ are piecewise linear, while the velocities $\boldsymbol{v}^{LB}$ are linear at the edges and piecewise constant in the element interiors. In the upper bound problem, the stresses $\boldsymbol{\sigma}^{UB}$ are instead linear at the edges and piecewise constant at the element interiors, while the velocities $\boldsymbol{v}^{UB}$ are piecewise linear. After applying such interpolations, the primal and dual problem in (1) and (2) turn into the following form,

$$\lambda^* = \max \lambda \qquad s.t. \begin{cases} \mathrm{A}\boldsymbol{\sigma}^{LB} + \lambda \mathrm{f} = 0 \\ \boldsymbol{\sigma}_i^{LB,e} \in \mathcal{B}, \qquad e = 1,\ldots,N_e, i = 1,\ldots,n_{sd}+1 \end{cases}$$

$$\lambda^* = \min_{\boldsymbol{v}} D(\boldsymbol{v}^{UB}) \qquad s.t. \begin{cases} \ell(\boldsymbol{v}^{UB}) = 1 \\ -\varepsilon(\boldsymbol{v}_i^{UB,e}) \in \mathcal{B}^*, \quad e = 1,\ldots,N_e, i = 1,2 \\ -[\![\boldsymbol{v}^{UB}]\!]_i^{\xi} \bar{\otimes} \boldsymbol{n}^{\xi} \in \mathcal{B}^*, \quad \xi = 1,\ldots,N_{\xi}, i = 1,2 \end{cases}$$

These problems can be solved efficiently using available optimisation programs. Moreover, usual plasticity criteria such as von Mises or Mohr-Coulomb in two dimensions allow us to rewrite the membership conditions as second order cones (SOC), which can be handled by the mentioned optimisation software. The optimum values of the lower and upper bound problem can be used to compute a set of elemental and edge contributions to the total gap, which are defined by:

$$\Delta\lambda^e = \int_{\Omega^e} \boldsymbol{\sigma}^{UB,e} : \varepsilon(\boldsymbol{v}^{UB}) d\Omega + \int_{\Omega^e} \nabla \cdot \boldsymbol{\sigma}^{LB} \cdot \boldsymbol{v}^{UB} d\Omega - \int_{\partial\Omega^e} \boldsymbol{\sigma}^{LB} \boldsymbol{n} \cdot \boldsymbol{v}^{UB} d\Gamma$$
$$\Delta\lambda^{\xi} = \int_{\Gamma^{\xi}} \boldsymbol{s}^{UB,\xi} \cdot [\![\boldsymbol{v}^{UB}]\!] d\Gamma - \int_{\Gamma^{\xi}} \boldsymbol{\sigma}^{LB} \boldsymbol{n} \cdot [\![\boldsymbol{v}^{UB}]\!] d\Gamma$$

These bound gaps satisfy the properties, $\lambda^{UB} - \lambda^{LB} = \Delta\lambda^e + \Delta\lambda^{\xi}$, $\Delta\lambda^e \geq 0$, $\Delta\lambda^{\xi} \geq 0$, which make them good candidates to estimate the errors of the lower and upper bound solution. We have used them to design an adaptive remeshing strategy.

3. EXTENSION TO INTERFACES, DUPLICATED EDGES AND JOINTS

We will develop next specific conditions for common interface conditions encountered in geomechanics. The conditions are:

1. **Interface material:** when two different materials are encountered, the practitioner must specify the admissibility criterion for the interface between these two materials. Computationally, these conditions are set by adding the following constraints:
    a. *Lower Bound:* New nodal stresses are defined at the interface, with the corresponding interface admissibility conditions, together with the equilibrium conditions between interface and edge stresses:

$$\begin{aligned} &\sigma_i^I \in \mathcal{B}_I, \quad i=1,2 \\ &(\sigma_i^A - \sigma_i^B)n = 0, \quad i=1,2 \\ &(\sigma_i^A - \sigma_i^I)n = 0, \quad i=1,2 \end{aligned} \tag{3}$$

    b. *Upper Bound*: It is sufficient to assign to the edge stresses the membership condition given in (3).
2. **Duplicated edges:** in two-dimensional applications, it may convenient to overlap materials or structural elements such as ties or anchors. In these situations, it is required to have edges that joint one element on one side (element *A*) and two elements, *B* and *B'*, on the other side. The equilibrium condition (lower bound) and exact kinematic conditions are then given by:
    a. *Lower Bound:* The exact equilibrium condition is now imposed witht he following equation:

$$(\sigma_i^A - \sigma_i^B - \sigma_i^{B'})n = 0, i = 1,2$$

    b. *Upper Bound*: The dissipation power and the admissibility condition for the edge stresses $\boldsymbol{s}^{\mathrm{UB}}$ now read,

$$b_\xi(s,v) = \int_{\Gamma^\xi} s^{A-B} \cdot (v^B - v^A) \mathrm{d}\Gamma + \int_{\Gamma^\xi} s^{A-B'} \cdot (v^{B'} - v^A) \mathrm{d}\Gamma$$

$$\left\{ \begin{array}{l} s_i^{A-B} \in \mathcal{B} \\ s_i^{A-B'} \in \mathcal{B} \end{array} \right. , i = 1,2,$$

3. **Modelling of joints:** The presence of punctual loads or the presence of articulated jonts require the modelling of joints. They can be represented in the optimisation problem by adding the following conditions:
    a. *Lower Bound:* The equilibrium conditions are not nodal but averaged throughout the edge:

$$\int (\sigma^A - \sigma^B) n \mathrm{d}\Gamma = 0$$

    b. *Upper Bound*: The linear relationship throughout the edge is equivalent to the follow condition,

$$[\![v]\!]_1 + [\![v]\!]_2 = 0$$

4. RESULTS

The extensions described so far have been employed to numerically test pull out capacity of multi-belled anchors. Figure 1(a) shows the contour plot of the dissipation energy for the upper bound solution. The linearity of the limit tension with respect to the number of bells has been verified. Five different anchor/soil conditions have been employed: rough (same properties as the soil), smooth (no resistance to shear), no tension condition, rough condition with no tension, and smooth condition with no-tension. Although the mechanisms do not significantly depend on these conditions, the pull out capacity does, and has been shown to be much larger for rough conditions.

The material properties have been shown to strongly influence the failure mechanism. While for clay materials (zero internal friction angle, but non-zero cohesion) the failure mechanism is localised around the anchor (see Figure 1(a)), in other sand materials the slide-lines propagate up to the soil surface. Further results have been reported in [3].

The model has been also applied to determine the maximum height of simply supported and anchored retaining walls. The limiting height has been compared with experimental results and other numerical models that use incremental plasticity. The agreement between our results and t the results has been very satisfactory [3]

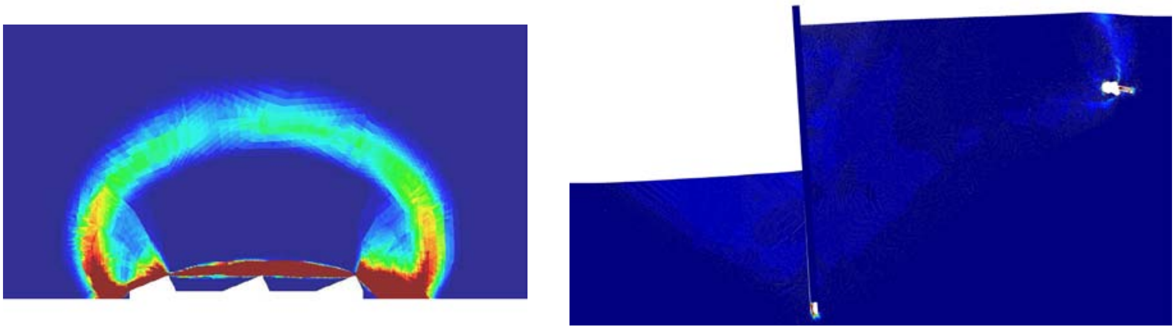

(a) (b)

Figure 1. Detail of anchor with three beels pulled from the left in clay material

5. CONCLUSIONS

This work has extended the applicability of computational limit analysis to practical problems. The agreement between our numerical results and the experimental values reported in the literature demonstrates the validity of the approach.

Further extensions to other geometries of anchors, soil stability or cavern securing in two and three dimensions can be analysed using the same ideas described here. The inclusion of pre-stressed anchors can be equally handled by modifying the equilibrium conditions or the dissipation energy. These further developments are currently under study.

The computation of bounds of the load factor for non-associative plasticity is also currently being investigated. Recent advances along this research line will be also presented.

RFERENCES

[1] W F Chen. Limit analysis and soil plasticity. Dev. in Geoth. Engin. 7. Elsevier, 1975.

[2] H Ciria, J Peraire, and J Bonet. Mesh adaptive computation of upper and lower bounds in limit analysis. Int. J.Num. Meth. Engng., 75:899–944, 2008.

[3] J J Muñoz, A V Lyamin, A Huerta. Stability of anchored sheet wall in cohesive-frictional soils by FE limit analysis. Submitted.